Electronic Supplementary Material (ESI) for Dalton Transactions.

Experimental and Theoretical Investigation of Four 3*d*−4*f* Butterfly Single-Molecule Magnets

Hua-Hong Zou [a], Liang-Bing Sheng [a], Fu-Pei Liang [a,c,*] Zi-Lu Chen [a], Yi-Quan Zhang [b,*]

[a]*Key Laboratory for the Chemistry and Molecular Engineering of Medicinal Resources (Ministry of Education of China), School of Chemistry & Pharmacy of Guangxi Normal University, Guilin 541004, P. R. China. E-mail: fliangoffice@yahoo.com*

[b]*Jiangsu Key Laboratory for NSLSCS, School of Physical Science and Technology, Nanjing Normal University, Nanjing 210023, P. R. China. E-mail: zhangyiquan@njnu.edu.cn*

[c]*Guangxi Key Laboratory of Electrochemical and Magnetochemical Functional Materials, College of Chemistry and Bioengineering, Guilin University of Technology, Guilin 541004, China*

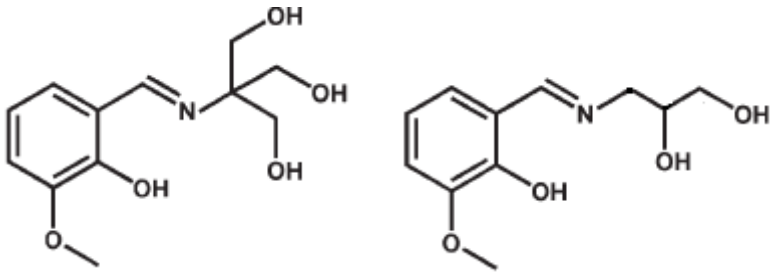

Scheme S1. Schiff base ligands H_4L_1 (left) and H_3L_2 (right).

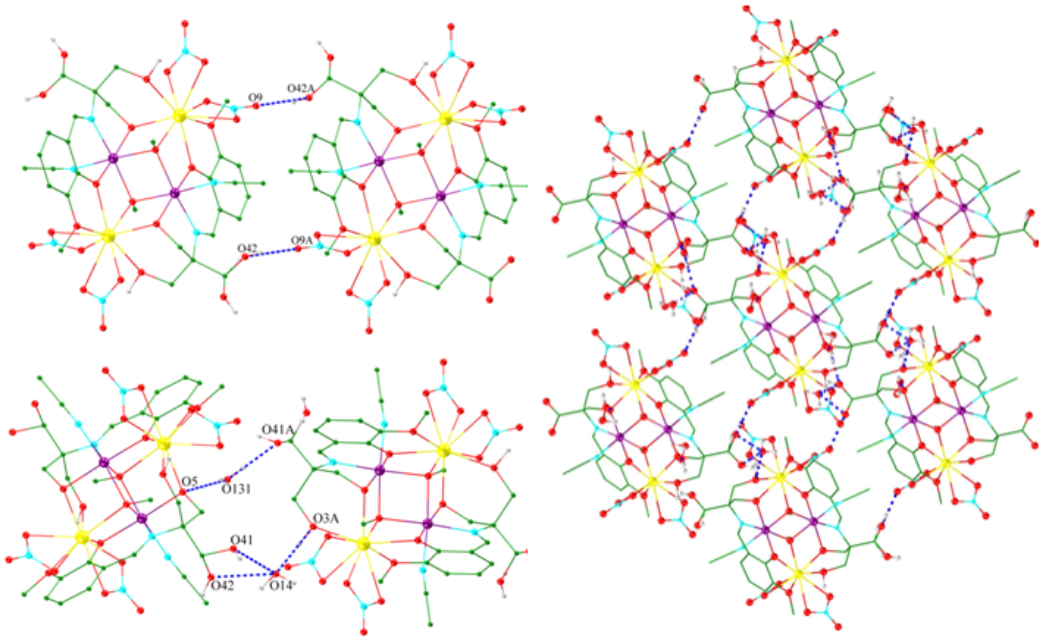

Fig. S1. The hydrogen-bonded interaction of adjacent clusters (left) and 2D layer (right) of complex **1**. Part of non-coordinated solvent molecules and hydrogen atoms are omitted for clarity. Color code: Ni, purple; Dy, yellow; O, red; N, light blue; C, green; H, gray.

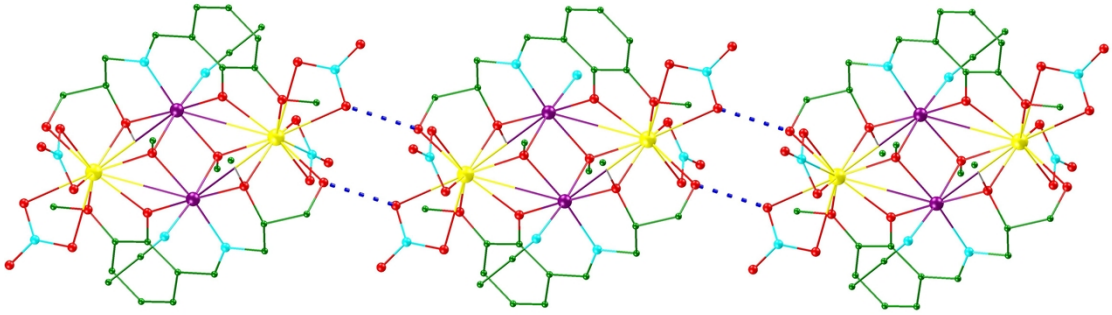

Fig. S2. The hydrogen-bonded interaction of adjacent clusters of complex **2** along the *c*-axis. The non-coordinated solvent molecules and the hydrogen atoms are omitted for clarity. Color code: Ni, purple; Dy, yellow; O, red; N, light blue; C, green.

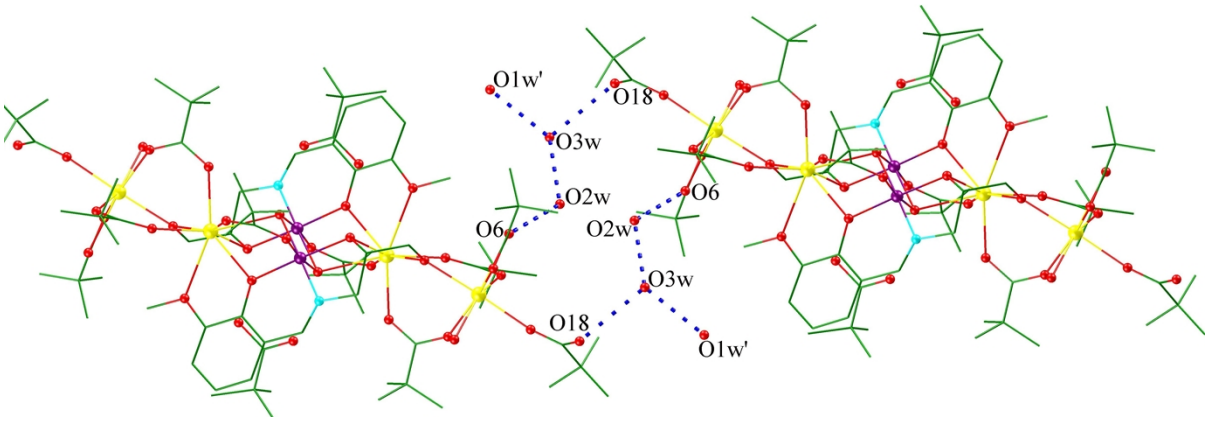

Fig. S3. The hydrogen-bonded interaction of adjacent clusters of complex **4** along the *b*-axis. The hydrogen atoms are omitted for clarity. Color code: Ni, purple; Dy, yellow; O, red; N, light blue; C, green; H, gray.

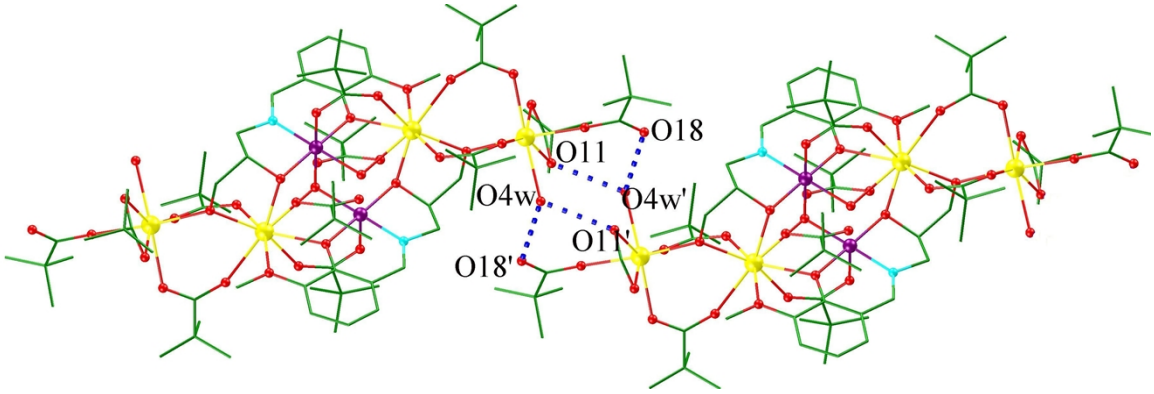

Fig. S4. The hydrogen-bonded interaction of adjacent clusters of complex **4** along the *c*-axis. The hydrogen atoms are omitted for clarity. Color code: Ni, purple; Dy, yellow; O, red; N, light blue; C, green; H, gray.

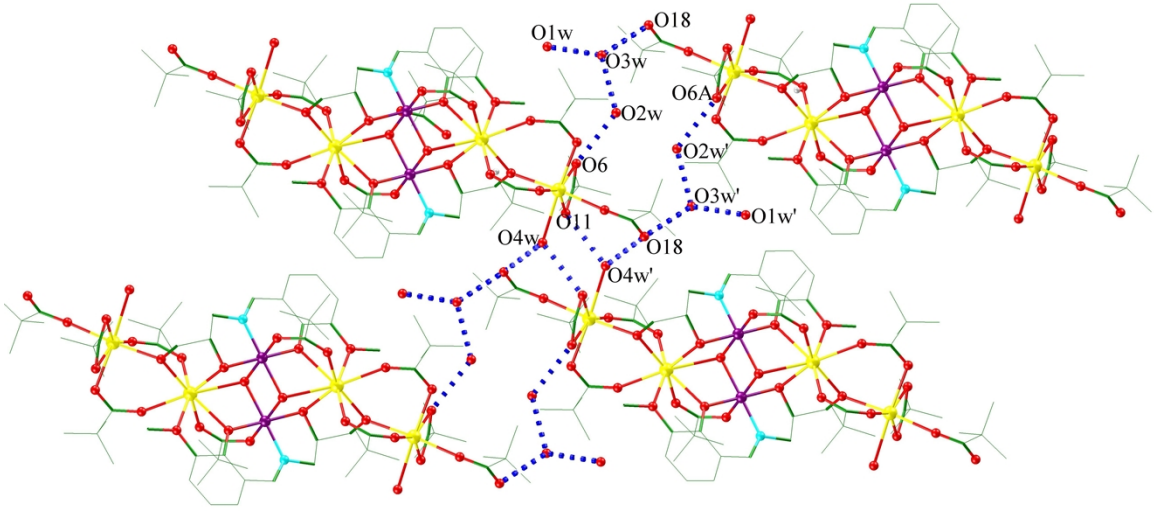

Fig. S5. The 2D hydrogen-bonded sheet of complex **4**. The hydrogen atoms are omitted for clarity. Color code: Ni, purple; Dy, yellow; O, red; N, light blue; C, green; H, gray.

Table S1. Hydrogen bond lengths (Å) and angles (°) for complex **1**.

D–H···A	*d*(D–H)	*d*(H···A)	*d*(D···A)	∠(DHA)	Symmetry codes
O42–H42A···O9	0.9700	1.8200	2.620(10)	138.00	1/2-x,1/2+y,3/2-z
O5–H5A···O131	0.8500	2.2400	3.023(11)	154.00	-1/2+x,3/2-y,1/2+z
O131–H131···O41	0.8400	2.0200	2.704(10)	138.00	3/2-x,-1/2+y,3/2-z
O14–H14A···O41	0.8500	2.2200	3.086(10)	156.00	1-x,2-y,1-z
O14–H14A···O42	0.8500	2.2200	3.121(10)	142.00	1-x,2-y,1-z
O14–H14B···O3A	0.8500	2.2200	3.220(10)	161.00	1/2-x,1/2+y,3/2-z

Table S2. Hydrogen bond lengths (Å) and angles (°) for complex **2**.

D–H···A	*d*(D–H)	*d*(H···A)	*d*(D···A)	∠(DHA)	Symmetry codes
O1–H1A···O5	0.8500	1.9700	2.781(10)	162.00	x, y, −1+z

Table S3. Hydrogen bond lengths (Å) and angles (°) for complex **3**.

D–H···A	*d*(D–H)	*d*(H···A)	*d*(D···A)	∠(DHA)	Symmetry codes
O1–H1A···O7	0.6800	2.1100	2.786(10)	172.00	x, y, −1+z

Table S4. Hydrogen bond lengths (Å) and angles (°) for complex **4**.

D–H···A	*d*(D–H)	*d*(H···A)	*d*(D···A)	∠(DHA)	Symmetry codes
O1w–H1w···O3w	0.9600	1.8500	2.860(10)	145.00	1−x, −y, 1−z
O2w–H2w···O3w	0.8500	2.2100	3.018(10)	156.00	1−x, 1−y, 1−z
O3w–H3w···O18	0.8500	2.0500	2.995(10)	148.00	x, −1+y, z
O2w–H2w···O6	0.8500	2.2100	3.036(10)	159.00	1−x, 1−y, 1−z
O4w–H4w···O18	0.8500	2.2000	3.109(10)	152.00	1-x,2-y,1-z
O4w–H4w···O11	0.8500	2.2000	3.205(10)	163.00	1-x,2-y,1-z

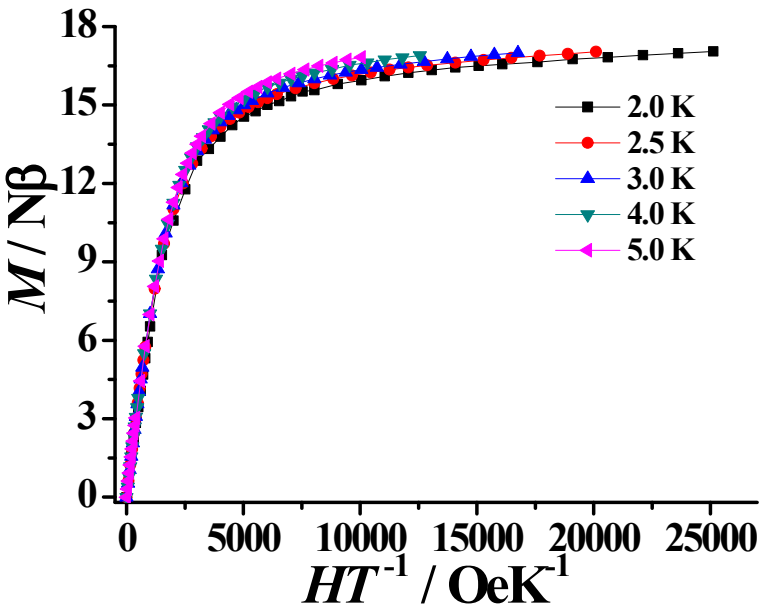

Fig. S6. *M* vs. *H/T* plot at various temperatures between 2 and 5 K for complex **1**.

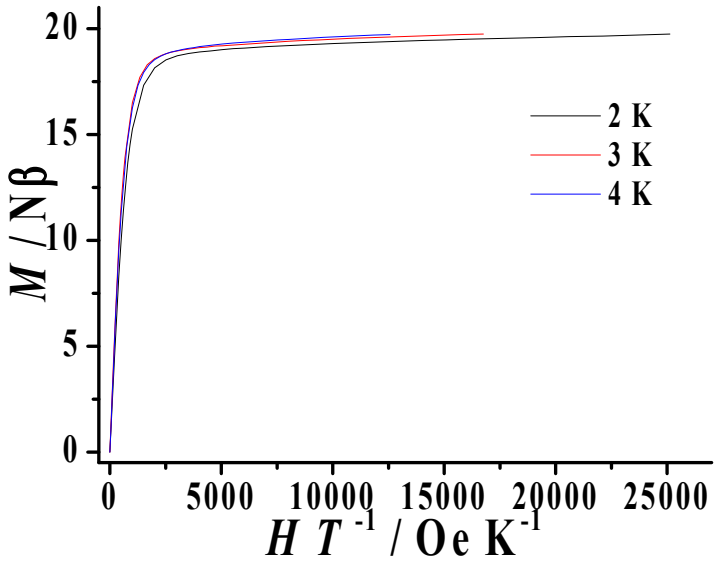

Fig. S7. *M* vs. *H/T* plot at various temperatures between 2 and 8 K for complex **2**.

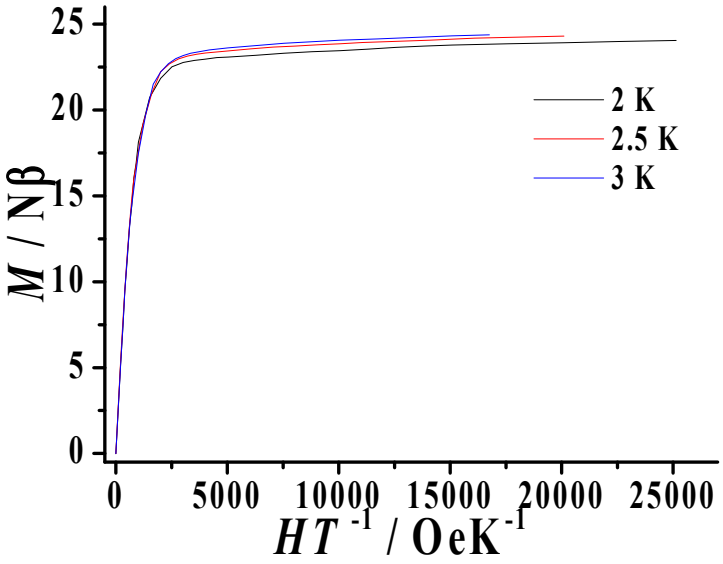

Fig. S8. *M* vs. *H/T* plot at various temperatures between 2 and 8 K for complex **3**.

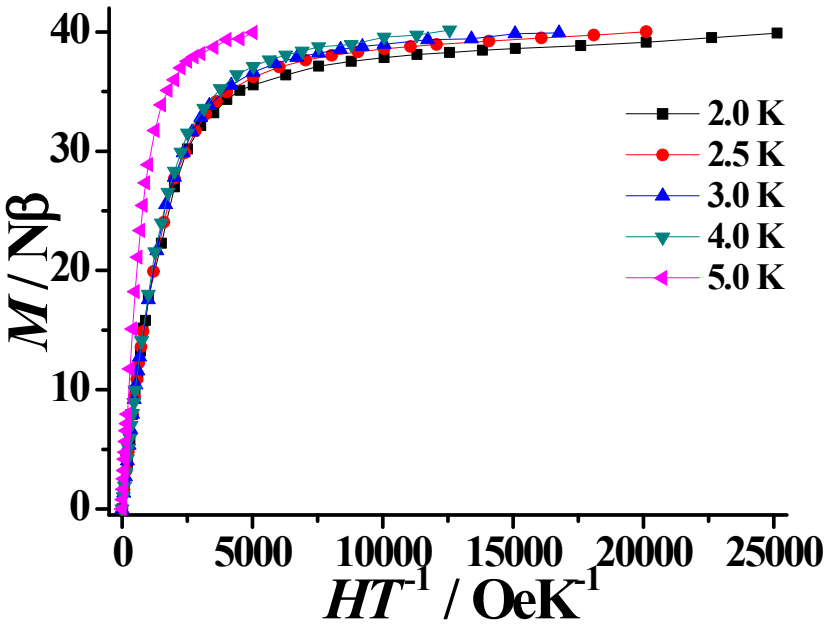

Fig. S9. *M* vs. *H/T* plot at various temperatures between 2 and 5 K for complex **4**.

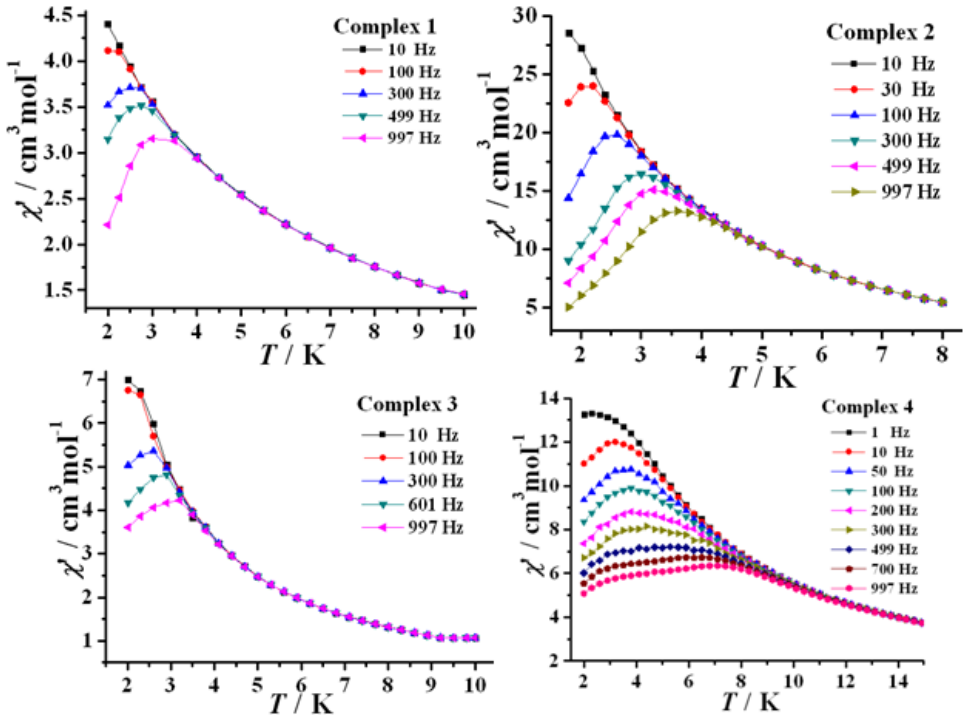

Fig. S10. Temperature dependent in-phase ac susceptibility for **1-4** in the absence of a dc field (H_{ac} = 2.5 Oe).

Table S5. Comparison of the ac magnetic data for 3*d*-4*f* complexes with butterfly topology (the 3*d* ions occupy the vertices of the body positions of the butterfly).

Complexes	detectable χ'' signal	T_b	Δ (K) and τ_0 (s) under H_{dc} (Oe)	References
$Ni^{II}_2Dy^{III}_2$(DMF)	yes	3.2 K, 1500 Hz	18.5, 5.4×10^{-7}, $H_{dc}=0$	21(a)
$Ni^{II}_2Tb^{III}_2$(DMF)	no	well below 1.8 K		21(a)
$Ni^{II}_2Dy^{III}_2$(MeOH)	yes	4.2 K, 1500 Hz	21.3, 1.5×10^{-6}, $H_{dc}=0$	21(a)
$Ni_2Tb^{III}_2$(MeOH)	yes	well no		21(a)
$Co^{II}_2Dy^{III}_2$		3.0 K	15.82, 7.7×10^{-4}; $H_{dc}=0$; 118.06, 6.2×10^{-7}, $H_{dc}=0$	19(a)
$Fe^{III}_2Ln^{III}_2$	yes	2.8 K, 200 Hz	16.21, 1.9×10^{-6}, $H_{dc}=1500$	19(c)
$Mn^{III}_2Dy^{III}_2$	yes		15, 3.31×10^{-7}, $H_{dc}=0$	19(f)
$Mn^{III}_2Dy^{III}_2$	no	well below 2 K		19(g)
$Mn^{III}_2Tb^{III}_2$	no	well below 2 K		19(g)
$Fe^{III}_2Ho^{III}_2$	no	0.3 K		19(d)
$Fe^{III}_2Dy^{III}_2$	no	1.1 K		19(d).
$Mg^{II}_2Dy^{III}_2$	yes	7.5 K, 1200 Hz	44, 7.8×10^{-7}, $H_{dc}=0$	19(h)
$Mg^{II}_2Er^{III}_2$	yes	4.0 K, 1200 Hz	23, 6.6×10^{-7}, $H_{dc}=0$	19(h)
$Ni^{II}_2Dy^{III}_2$	yes	3.5 K, 1200 Hz	20, 6×10^{-7}, $H_{dc}=0$	19(h)
$Ni^{II}_2Dy^{III}_2$	yes	4.3 K, 1000 Hz	48.46, 3.6×10^{-8}, $H_{dc}=0$	This work.
$Ni^{II}_2Tb^{III}_2$	yes	3.2 K, 1000 Hz	86.71, 2.3×10^{-7}, $H_{dc}=0$	This work.
$Ni^{II}_2Dy^{III}_2$	yes	4.5 K, 1000 Hz	56.94, 3.3×10^{-8}, $H_{dc}=0$	This work.
$Co^{III}_2Dy^{III}_2$	yes	4.8 K, 1000 Hz	26.46, 8.7×10^{-6}, $H_{dc}=0$	This work.

T_b is the blocking temperature; Δ is the energy gap to the reversal of magnetization; τ_0 is the relaxation time.

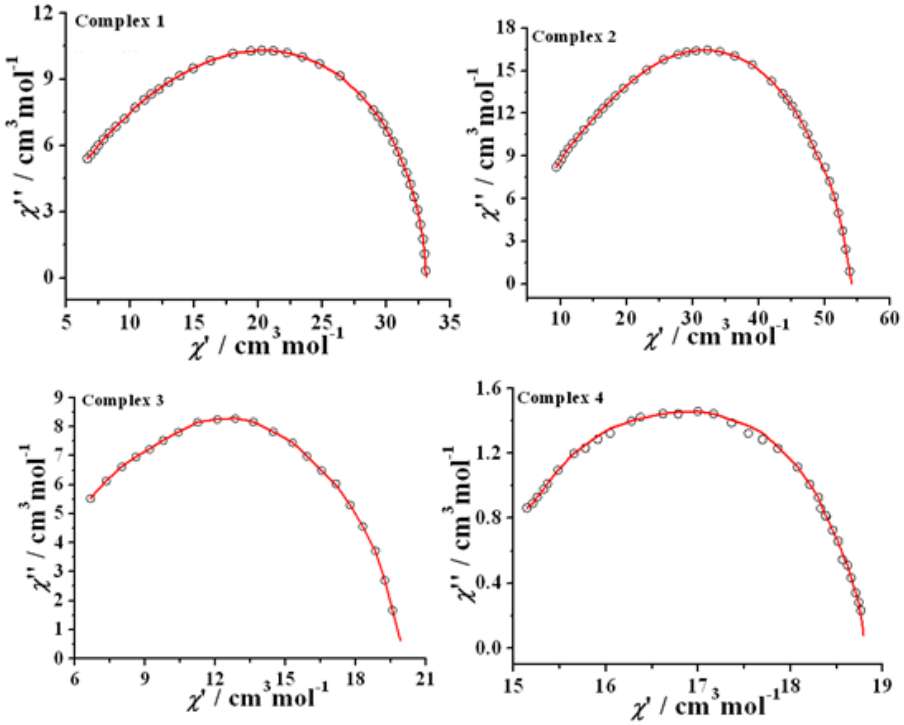

Fig. S11. Cole-Cole diagram of **1-4** at 2 K with zero dc field. The solid lines represent the best fitting of the experimental data to the generalized Debye model.

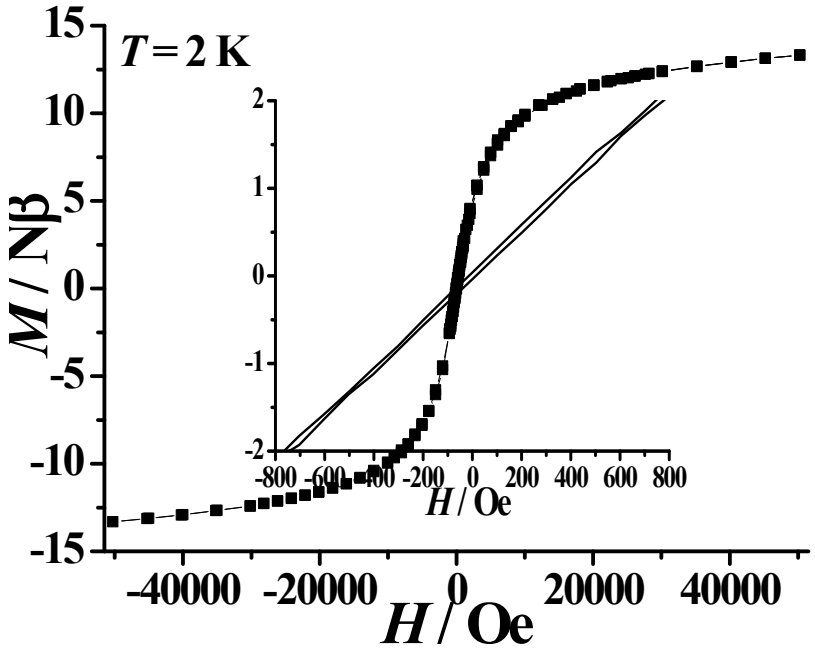

Fig. S12. Magnetic hysteresis loop of **1** recorded at 2 K, the inset shows a zoom around zero field.

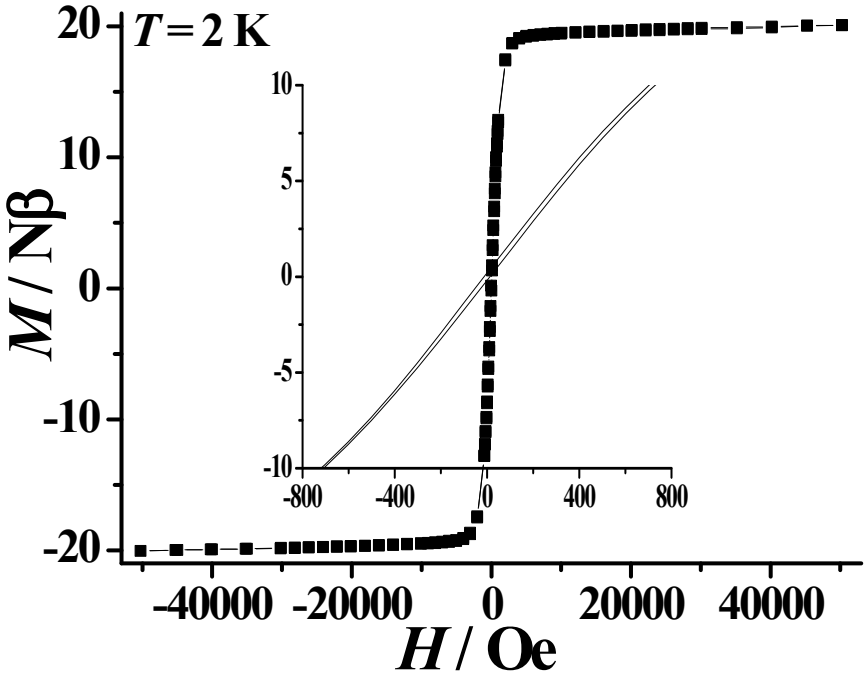

Fig. S13. Magnetic hysteresis loop of **2** recorded at 2 K, the inset shows a zoom around zero field.

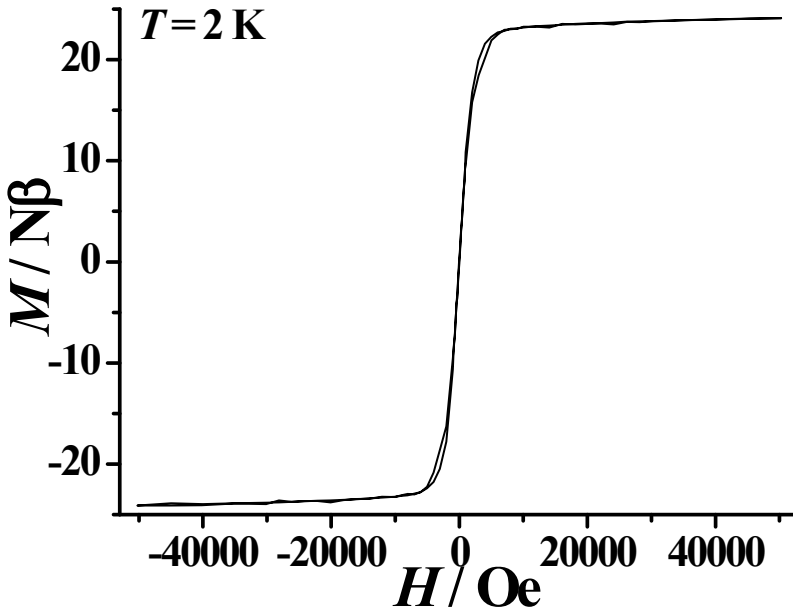

Fig. S14. Magnetic hysteresis loop of **3** recorded at 2 K.

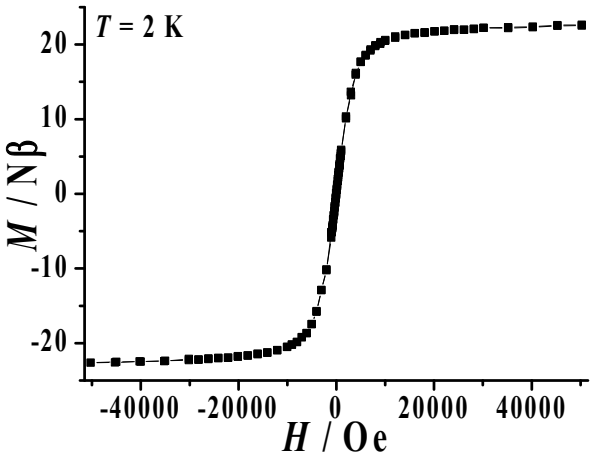

Fig. S15. Magnetic hysteresis loop of **4** recorded at 2 K, the inset shows a zoom around zero field.

Table S6. Energies (cm^{-1}) and ***g*** (g_x, g_y, g_z) tensors of the lowest spin-orbit states on the Dy^{III} or Tb^{III} fragments of **1**–**4**.

1		**2**		**3**		**4**			
						a		***b***	
E	***g***	*E*	***g***	*E*	***g***	*E*	***g***	*E*	***g***
0.0	0.025	0.0	0.000	0.0	0.003	0.0	0.008	0.0	0.372
	0.041	0.0	0.000		0.010		0.011		0.801
	19.708		17.868		19.484		19.837		18.784
157.2	0.613	164.4	0.000	164.5	1.484	305.2	0.9597	59.5	2.501
	1.093	166.7	0.000		3.746		2.2435		5.124
	16.450		15.072		13.914		15.388		11.485
204.9	0.259	238.9	0.000	188.2	1.349	369.9	0.511	103.1	8.394
	1.980	245.4	0.000		3.331		2.427		5.279

	16.434		11.149		11.483		15.492		0.634
277.0	4.713	322.6	0.000	251.1	1.845	458.1	1.624	142.6	0.704
	6.421	345.0	0.000		3.184		3.319		3.120
	9.908		7.572		15.319		13.849		13.833
351.6	0.669	322.6	0.000	286.7	1.660	516.4	1.328	198.2	8.470
	4.176	(*m*$_J$=0)	0.000		5.556		3.858		7.309
	11.910		9.019		9.767		9.454		4.060
390.3	1.372	345.0	0.000	370.8	0.499	548.2	3.807	272.2	0.679
	2.054	354.8	0.000		3.613		4.833		0.984
	10.108		2.890		10.691		9.061		14.005
424.0	0.064	405.4	0.000	448.6	1.541	606.2	1.160	389.5	0.306
	1.437	422.0	0.000		2.248		3.416		0.425
	13.385		0.741		13.36913		11.625		17.828
523.0	0.161	471.8	0.000	506.5	0.497	674.1	0.195	548.0	0.017
	0.372	478.9	0.000		1.200		0.851		0.039
	18.785		3.868		17.529		17.671		19.486

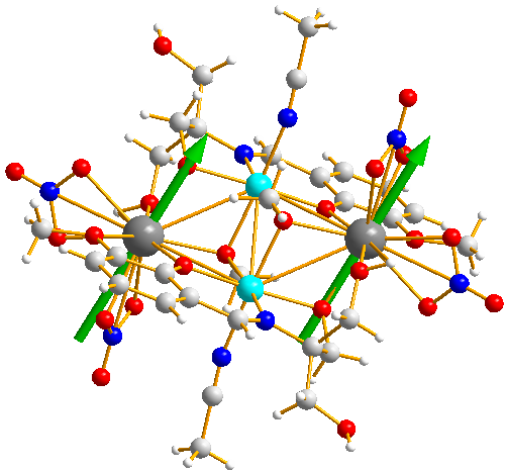

Complex 1

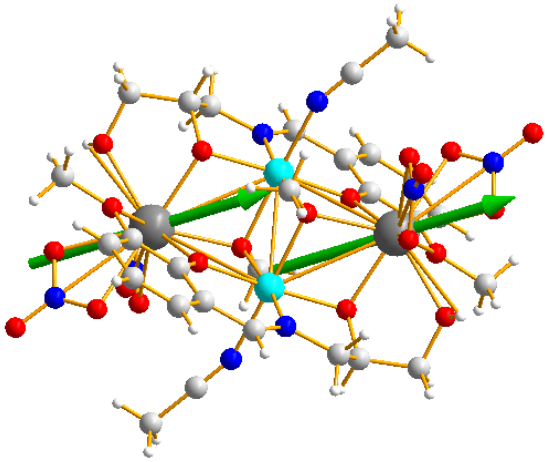

Complex 2

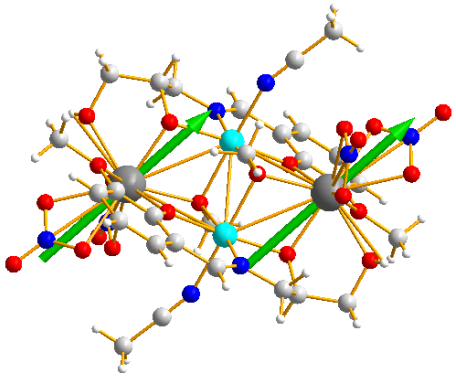

Complex 3

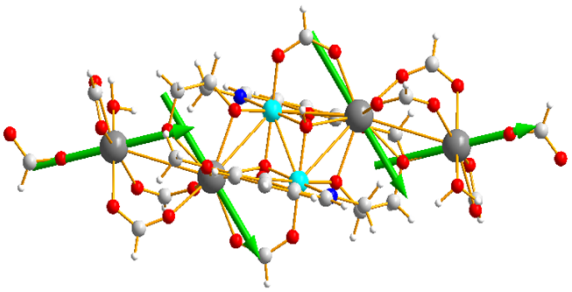

Complex 4

Fig. S16. Orientations of the local main magnetic axes of the ground doublets on Dy^{III} or Tb^{III} ions of **1**−**4**.

Estimation of the exchange interactions in four complexes by BS-DFT

calculation

To obtain the isotropic exchange coupling constants *J*, Orca 2.9.1 calculations[1] were performed with the popular hybrid functional B3LYP proposed by Becke[2-3] and Lee et al.[4] Triple-ζ with one polarization function TZVP[5-6] basis sets were used for all atoms, and zero order regular approximation (ZORA) was used for the scalar relativistic effect in all calculations. For complexes **1**, **2** and **3**, the nearest neighboring Ln-Ni^{II} and Ni^{II}-Ni^{II} exchange interactions and the next neighboring Ln-Ln couplings were all considered. For **4**, only the nearest Dy^{III}-Dy^{III} interactions were considered. We firstly used the isotropic Gd^{III} ions to replace Dy^{III} or Tb^{III} ions to calculate the exchange couplings, and then the obtained exchange parameters corresponding to Gd^{III}-Ni^{II} and Gd^{III}-Gd^{III} were re-scaled for the interacting pairs of Dy^{III}-Ni^{II}, Tb^{III}-Ni^{II}, Dy^{III}-Dy^{III} and Tb^{III}-Tb^{III}, respectively.[7] The large integration grid (grid = 6) was applied to Gd^{III} and Ni^{II} for ZORA calculations. Tight convergence criteria were selected to ensure the results to be well converged with respect to technical parameters. For complexes **1**, **2**, and **3**, through calculating the energies of four spin states: the high-spin state ($S_{HS} = S_{Gd1}+S_{Ni1}+S_{Ni2}+S_{Gd2}$), the first broken-symmetry (BS) state (flip the spins on two Ni^{II}; $S_{BS1} = S_{Gd1}-S_{Ni1}-S_{Ni2}+S_{Gd2}$), the second BS state (flip the spins on one Ni^{II}; $S_{BS2} = S_{Gd1}+S_{Ni1}-S_{Ni2}+S_{Gd2}$), and the third BS state (flip the spins on one Gd^{III}; $S_{BS3} = S_{Gd1}+S_{Ni1}-S_{Ni2}-S_{Gd2}$), the isotropic Gd^{III}-Gd^{III}, Gd^{III}-Ni^{II}, Ni^{II}-Ni^{II} coupling constants $J_{Gd\text{-}Gd}$, $J_{Gd\text{-}Ni}$ and $J_{Ni\text{-}Ni}$ were obtained by eqs **1–3** deduced using the spin-projected approach.[8-10]

$$J_{Gd-Gd} = \frac{E_{BS3} - E_{HS}}{28} \quad (1)$$

$$J_{Gd-Ni} = \frac{E_{BS1} - E_{HS}}{30} \quad (2)$$

$$J_{Ni-Ni} = \frac{E_{BS2} - E_{HS} - 14J_{Gd-Ni}}{3} \quad (3)$$

For complex **4**, two spin states were calculated to obtain the constant $J_{Gd\text{-}Gd}$: the high-spin state ($S_{HS} = S_{Gd1}+S_{Gd2}+S_{Gd3}+S_{Gd4}$), the first broken-symmetry state (flip the spins on two Gd^{III}; $S_{BS} = S_{Gd1}-S_{Gd2}-S_{Gd3}+S_{Gd4}$).

$$J_{Gd-Gd} = \frac{E_{BS} - E_{HS}}{56} \quad (4)$$

According to the rescaling equation proposed by Chibotaru and co-workers,[7] the corresponding $J_{\text{Dy-Ni}}$, $J_{\text{Tb-Ni}}$, and $J_{\text{Dy-Dy}}$ of complexes **1**, **2**, **3** and **4** are equal to $7/5J_{\text{Gd-Ni}}$, $7/6J_{\text{Gd-Ni}}$ and $(7/5)^2J_{\text{Gd-Gd}}$, respectively.

Fitting the exchange interaction in four complexes using Lines model based on CASSCF results

To fit the exchange interactions in four complexes, we took two steps to obtain them. Firstly, we calculated the mononuclear fragments using CASSCF to obtain the corresponding magnetic properties (see the first part). And then, the exchange interaction between the magnetic centers is considered within the Lines model,[11] while the account of the dipole-dipole magnetic coupling is treated exactly. The Lines model is effective and has been successfully used widely in the research field of 3*d*-4*f* single-molecule magnets.[12]

For complexes **1** and **3**, the exchange Hamiltonian is:

$$\hat{H}_{exch} = -J^{total}_{Dy-Ni}(\hat{S}_{Dy1}\hat{S}_{Ni1} + \hat{S}_{Dy1}\hat{S}_{Ni2} + \hat{S}_{Dy2}\hat{S}_{Ni1} + \hat{S}_{Dy2}\hat{S}_{Ni2}) - J^{total}_{Ni-Ni}\hat{S}_{Ni1}\hat{S}_{Ni2} - J^{total}_{Dy-Dy}\hat{S}_{Dy1}\hat{S}_{Dy2} \quad (5)$$

For complex **2**, the exchange Hamiltonian is:

$$\hat{H}_{exch} = -J^{total}_{Tb-Ni}(\hat{S}_{Tb1}\hat{S}_{Ni1} + \hat{S}_{Tb1}\hat{S}_{Ni2} + \hat{S}_{Tb2}\hat{S}_{Ni1} + \hat{S}_{Tb2}\hat{S}_{Ni2}) - J^{total}_{Ni-Ni}\hat{S}_{Ni1}\hat{S}_{Ni2} - J^{total}_{Tb-Tb}\hat{S}_{Tb1}\hat{S}_{Tb2} \quad (6)$$

For complex **4**, the exchange Hamiltonian is:

$$\hat{H}_{exch} = -J^{total}_{Dy-Dy}(\hat{S}_{Dy1}\hat{S}_{Dy2} + \hat{S}_{Dy3}\hat{S}_{Dy4}) \quad (7)$$

The J^{total}_{Dy-Ni}, J^{total}_{Ni-Ni}, J^{total}_{Tb-Ni}, and J^{total}_{Dy-Dy} are parameters of the total magnetic interaction ($J^{total} = J^{diploar} + J^{exchange}$) between magnetic center ions. The $\hat{S}_{Dy}$ = $\hat{S}_{Tb}$ = ±1/2 are the ground pseudospin on the Dy and Tb sites, and the $\hat{S}_{Ni}$ = 1 is the pseudospin of the Ni site. The dipolar magnetic coupling can be calculated exactly, while the exchange coupling constants were fitted through comparison of the computed and measured magnetic susceptibility and molar magnetization using the POLY_ANISO program.[13]

Table S7. Calculated energies (cm^{-1}), the corresponding tunneling gaps and the g_z values of the low-lying exchange doublet states of complexes **1**, **2**, **3** and **4**.

1			2			3			4		
E	Δ_{tun}	g_z	E	Δ_{tun}	g_z	E	Δ_{tun}	g_z	E	Δ_{tun}	g_z
0.00	2.4E-08	48.53	0.00	1.1E-07	44.86	0.00	2.9E-08	48.09	0.00	5.0E-06	0.00
22.56	9.7E-06	43.97	36.48	2.2E-06	40.30	20.07	1.3E-05	43.53	0.52	5.0E-06	65.78
35.04	9.8E-03	0.00	61.37	1.4E-02	34.10	40.32	8.1E-03	33.14	18.25	1.5E-05	42.93
35.06	4.9E-03	0.00	61.51	1.4E-02	0.00	40.33	5.2E-03	0.00	18.27	1.5E-05	42.92
35.16	1.1E-02	35.29	61.61	1.8E-05	0.00	40.39	3.1E-03	0.00	18.80	1.5E-05	0.00
35.23	4.4E-03	0.00	61.84	1.5E-05	0.00	40.52	1.2E-04	0.00	18.81	1.5E-05	0.00
35.33	2.6E-03	0.00	62.31	4.1E-05	0.00	40.78	4.3E-05	0.00	36.52	4.5E-05	0.00
35.36	5.4E-03	0.00	62.33	1.6E-05	0.00	40.79	1.4E-05	0.00	37.09	4.5E-05	45.58
47.80	2.6E-04	34.86	80.30	1.1E-06	40.30	60.78	3.7E-06	34.41			
60.48	1.5E-06	30.30	86.72	3.8E-05	31.17	63.48	4.4E-06	43.53			
67.08	3.3E-06	43.97	105.11	2.5E-02	31.08	81.43	7.2E-07	29.85			
79.61	2.9E-03	0.00	105.19	2.5E-02	0.00	83.70	2.4E-04	0.00			
79.64	5.0E-03	0.00	105.35	3.1E-06	0.00	83.76	1.3E-03	38.31			
79.71	5.7E-03	37.16	105.55	1.5E-05	0.00	83.80	1.4E-03	0.00			
79.85	3.4E-03	0.00	112.52	1.2E-06	26.61	83.96	1.4E-04	0.00			
92.31	8.7E-05	34.86	127.06	3.1E-02	29.13	104.20	1.2E-06	34.41			
101.95	8.5E-08	39.42	127.12	3.1E-02	0.00	105.46	8.7E-09	38.96			
101.98	4.3E-08	0.00	130.56	1.2E-05	31.17	105.50	3.2E-08	0.00			

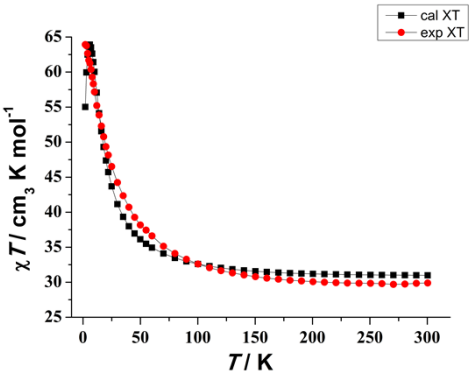

1

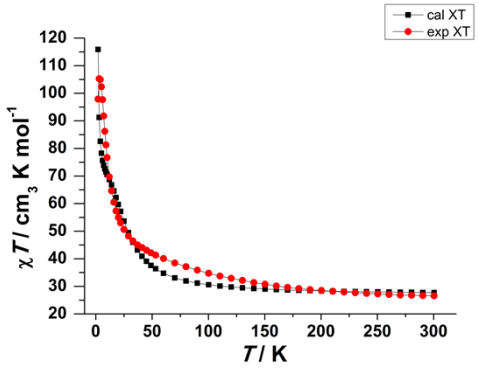

2

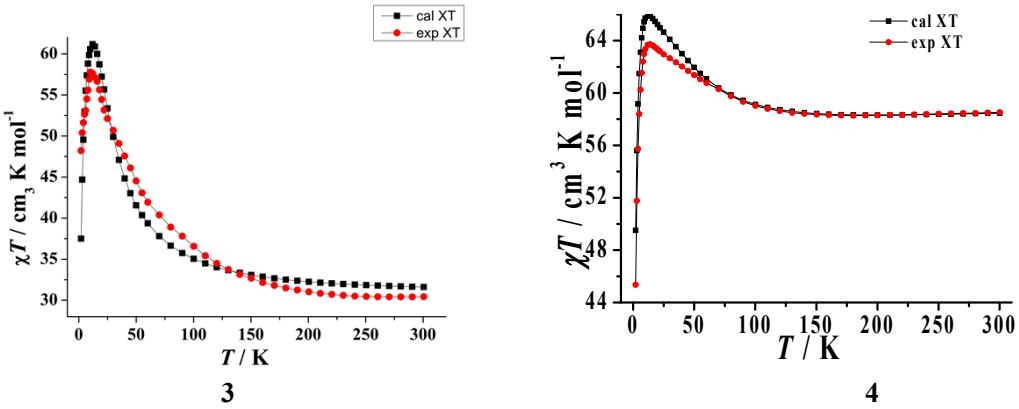

Fig. S17. Calculated and experimental data of magnetic susceptibility of complexes **1**–**4**.

The intermolecular interaction zJ' of **1**-**4** were set to –0.01 cm^{-1}, 0.01 cm^{-1}, –0.028 cm^{-1} and –0.01 cm^{-1}, respectively.

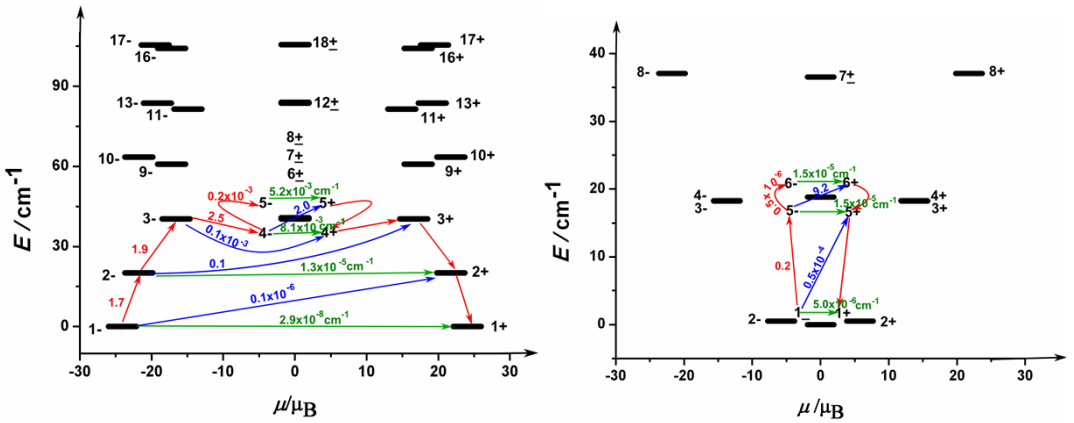

Fig. S18. The magnetization blocking barriers in complexes **3** (left) and **4** (right). The arrows show the connected exchange states. The numbers at each arrow stand for the mean absolute value of the corresponding matrix element of the transversal magnetic moment.

References:

(1) Neese, F. ORCA–*an ab initio, density functional and semiempirical program package*, version 2.9.1; Max-Planck institute for bioinorganic chemistry: Mülheim an der Ruhr, Germany, 2012.

(2) Becke, A. D. *J. Chem. Phys*. **1993**, *98*, 5648.

(3) Becke, A. D. *Phys. Rev. A*. **1988**, *38*, 3098.

(4) Lee, C.; Yang, W.; Parr, R. G. *Phys. Rev. B*. **1988**, *37*, 785.

(5) Schafer, A.; Horn, H.; Ahlrichs, R. *J. Chem. Phys*. **1992**, *97*, 2571.

(6) Schafer, A.; Huber, C.; Ahlrichs, R. *J. Chem. Phys*. **1994**, *100*, 5829.

(7) Vieru, V.; Ungur, L.; Chibotaru, L. F., *J. Phys. Chem. Lett*. **2013**, *4*, 3565.

(8) Noodleman, L. *J. Chem. Phys*. **1981**, *74*, 5737.

(9) Noodleman, L.; Baerends, E. J. *J. Am. Chem. Soc.* **1984**, *106*, 2316.

(10) Noodleman, L.; Case, D. A. *Adv. Inorg. Chem*. **1992**, *38*, 423.

(11) Lines, M. E. *J. Chem. Phys*. **1971**, *55*, 2977.

(12) (a) Mondal, K. C.; Sundt, A.; Lan, Y. H.; Kostakis, G. E.; Waldmann, O.; Ungur, L.; Chibotaru, L. F.; Anson, C. E.; Powell, A. K. *Angew. Chem. Int. Ed*. **2012**, *51*, 7550; (b) Langley, S. K.; Wielechowski, D. P.; Vieru, V.; Chilton, N. F.; Moubaraki, B.; Abrahams, B. F.; Chibotaru, L. F.; Murray, K. S. *Angew. Chem. Int. Ed*. **2013**, *52*, 12014.

(13) (a) Chibotaru, L. F.; Ungur, L.; Soncini, A. *Angew. Chem. Int. Ed.*, **2008**, *47*, 4126; (b) Ungur, L.; Van den Heuvel, W.; Chibotaru, L. F. *New J. Chem.*, **2009**, *33*, 1224; (c) Chibotaru, L. F.; Ungur, L.; Aronica, C.; Elmoll, H.; Pilet, G.; Luneau, D. *J. Am. Chem. Soc.*, **2008**, *130*, 12445.